© 2018. Published by The Company of Biologists Ltd | Development (2018) 145, dev158154. doi:10.1242/dev.158154

RESEARCH ARTICLE

Xenopus ADAM19 regulates Wnt signaling and neural crest specification by stabilizing ADAM13

Jiejing Li[1,2,*], Mark Perfetto[1,3,*], Russell Neuner[4], Harinath Bahudhanapati[1], Laura Christian[1], Ketan Mathavan[4], Lance C. Bridges[5], Dominique Alfandari[4] and Shuo Wei[3,‡]

ABSTRACT

During vertebrate gastrulation, canonical Wnt signaling induces the formation of neural plate border (NPB). Wnt is also thought to be required for the subsequent specification of neural crest (NC) lineage at the NPB, but the direct evidence is lacking. We found previously that the disintegrin metalloproteinase ADAM13 is required for Wnt activation and NC induction in *Xenopus*. Here, we report that knockdown of ADAM13 or its close paralog ADAM19 severely downregulates Wnt activity at the NPB, inhibiting NC specification without affecting earlier NPB formation. Surprisingly, ADAM19 functions nonproteolytically in NC specification by interacting with ADAM13 and inhibiting its proteasomal degradation. Ectopic expression of stabilized ADAM13 mutants that function independently of ADAM19 can induce the NC marker/specifier *snail2* in the future epidermis via Wnt signaling. These results unveil the essential roles of a novel protease-protease interaction in regulating a distinct wave of Wnt signaling, which directly specifies the NC lineage.

KEY WORDS: Neural crest, Neural plate border, Disintegrin metalloproteinase (ADAM), Wnt signaling, *Xenopus*

INTRODUCTION

The vertebrate neural crest (NC) cells are multipotent embryonic cells that give rise to the craniofacial cartilages and bones, sensory neurons and glia, pigment cells, cardiac tissues, and many other cells and tissues. Deficiencies in NC development are a major cause of human birth defects, ranging from relatively subtle craniofacial abnormalities to more severe diseases such as CHARGE and DiGeorge syndromes (Bronner and Simões-Costa, 2016; Mayor and Theveneau, 2013). NC-based cell therapies are also being developed to repair tissues that are damaged by injuries or deteriorate with age (Kunisada et al., 2014; Zhu et al., 2016). Understanding the basic mechanisms that control the specification of NC lineage is crucial for developing new methods to prevent NC-related birth defects and to regenerate NC-derived tissues for clinical applications.

[1]Department of Biology, West Virginia University, Morgantown, WV 26506, USA. [2]Department of Clinical Laboratory, The Affiliated Hospital of KMUST, Medical School, Kunming University of Science and Technology, Kunming 650032, China. [3]Department of Biological Sciences, University of Delaware, Newark, DE 19716, USA. [4]Department of Veterinary and Animal Sciences, University of Massachusetts, Amherst, MA 01003, USA. [5]Biochemistry, Molecular and Cell Sciences, Arkansas College of Osteopathic Medicine, Arkansas Colleges of Health Education, Fort Smith, AR 72916, USA.
*These authors contributed equally to this work

‡Author for correspondence (swei@udel.edu)

R.N., 0000-0002-9630-1478; S.W., 0000-0001-8203-4922

Received 8 August 2017; Accepted 29 January 2018

In vertebrate embryos, the NC cells are induced at the neural plate border (NPB) during gastrulation. NC induction requires coordinated actions of multiple signaling pathways, which activate the expression of transcription factors such as Pax3/7, Zic1 and Msx1 that induce NPB formation (i.e. the NPB specifiers). The NPB specifiers in turn activate the expression of another set of transcription factors (i.e. the NC specifiers), such as Snail2, FoxD3 and Sox9, which specify NC lineage in certain NPB cells. Once specified, the NC cells undergo proliferation while maintaining their multipotency. Around the time of neural tube closure, the NC cells delaminate and migrate to specific destinations, where they differentiate into various types of cells and tissues (Bronner and Simões-Costa, 2016; Simões-Costa and Bronner, 2015; Stuhlmiller and García-Castro, 2012).

A major signaling pathway that is essential for NC induction is the canonical Wnt pathway. In *Xenopus* embryos, Wnt seems to be important for both the initial formation of the NPB and the subsequent specification of NC lineage. During NPB formation, Wnt is required for inducing the expression of Pax3 and Msx1, which cooperate with Zic1 to set up the NPB (Li et al., 2009; Monsoro-Burq et al., 2005). Gain-of-function studies suggest that the combination of Pax3 and Zic1 is sufficient to specify the NC lineage *ex vivo* in the animal cap or ectopically in the ventral ectoderm, and this effect is again Wnt-dependent (Milet et al., 2013; Monsoro-Burq et al., 2005; Sato et al., 2005). The direct Wnt target in NC specification is probably Snail2, as *snail2* is the only NC specifier gene whose enhancer is known to contain a Wnt-responsive LEF/TCF-binding site (Simões-Costa and Bronner, 2015; Vallin et al., 2001). However, it remains unclear whether the specification of endogenous NC lineage also requires Wnt activity.

The disintegrin metalloproteinases (ADAMs) are multi-domain transmembrane proteins that play important roles in development and disease. Most of the functional domains of ADAMs are extracellular, including a metalloproteinase domain that is catalytically active in some but not all ADAMs, as well as disintegrin and cysteine-rich domains that can mediate protein-protein interactions (Wei, 2013). About half of the ADAMs are expressed predominantly in the testis and are mainly involved in reproduction, whereas the others have significant presence in somatic tissues. Several somatic ADAMs are known to control cell signaling through their protease activities. For example, proteolytic processing of the Notch receptors by ADAM10 is necessary for Notch signal activation, and shedding of the ligands for epithelial growth factor receptors (EGFRs) by multiple ADAMs is an essential regulatory event in EGFR signaling (Edwards et al., 2008; Reiss and Saftig, 2009). We have also shown that another ADAM, ADAM13, induces NC in *Xenopus* embryos by regulating canonical Wnt signaling. Knockdown (KD) of ADAM13 leads to reduced expression of markers for pre-migratory NC and inhibition of Wnt8-induced axis duplication. We further identified ephrin B1

Development (2018) 145, dev158154. doi:10.1242/dev.158154

and ephrin B2, two cell-surface ligands for EphB receptor tyrosine kinases, as the *in vitro* and *in vivo* substrates for ADAM13 and antagonists of Wnt signaling. By cleaving these ephrins, ADAM13 permits Wnt activation, which in turn induces the NC (Wei et al., 2010b). Although these results clearly demonstrate the importance of ADAM13 in Wnt signaling and NC induction, direct evidence showing the regulation of endogenous Wnt signaling by ADAM13 in one or both stages of NC induction was still missing.

In the current study, we have investigated further the roles of ADAM13 and its close paralog ADAM19 in Wnt signaling and NC induction in *X. tropicalis* embryos. Using a transgenic Wnt reporter line, we detected high endogenous Wnt activity at the NPB at late gastrula stages. KD of either ADAM13 or ADAM19 caused strong inhibition of Wnt activity at the NPB and reduced expression of NC markers; however, the expression of NPB markers remained unaffected. Thus, ADAM13 and ADAM19 are both required for a particular wave of Wnt signaling that directly specifies the NC lineage but is not required for NPB formation. We further show that the function of ADAM19 in NC specification is independent of its protease activity but via protection of ADAM13. ADAM13 and ADAM19 colocalized in the ER and physically interacted with each other, and KD of ADAM19 resulted in reduction of ADAM13 protein levels that was caused by proteasomal degradation. Such proteasomal degradation was mediated by a conserved C-terminal lysine residue of ADAM13, as mutation of this lysine residue to arginine or deletion of the whole cytoplasmic tail generated stabilized ADAM13 mutants that were resistant to ADAM19 KD. Ectopic expression of these stabilized ADAM13 mutants could not only rescue the NC specification defects caused by ADAM19, but also induce robust expression of *snail2* in the future epidermis in a Wnt-dependent manner. Together, our data suggest a novel non-proteolytic function of ADAM19 in regulating the turnover of ADAM13 and a distinct wave of Wnt signaling that specifies the NC lineage.

RESULTS

Knockdown of ADAM19 phenocopies ADAM13 loss of function in *X. tropicalis* embryos

Our phylogenetic and syntenic (gene linkage) analyses suggest that ADAM12, ADAM13 and ADAM19 form a subfamily of proteolytically active ADAMs that is conserved among vertebrates (note that the mammalian ortholog of *Xenopus* ADAM13 is ADAM33) (Bahudhanapati et al., 2015; Wei et al., 2010a). Similar to its *X. laevis* ortholog (Neuner et al., 2009), *X. tropicalis adam19* was found to be expressed in the dorsal mesoderm during mid-gastrulation, and broadly in the dorsal ectoderm at the end of gastrulation (Fig. S1A,B). At the same stages, transcripts of *adam13* were detected in the mesoderm and pre-migratory NC, respectively (Wei et al., 2010b). By contrast, *adam12* did not display any specific expression patterns (data not shown).

We reported previously that KD of ADAM13 causes defects in craniofacial and eye development in *X. tropicalis* embryos (Wei et al., 2012, 2010b). To understand the functions of ADAM12 and ADAM19, antisense MOs were designed to block the translation of individual ADAMs (Fig. 1A) (Wei et al., 2010b). Morphology of the craniofacial structures was characterized using a transgenic *X. tropicalis* reporter line that expresses enhanced green fluorescent protein (eGFP) driven by a ∼4 kb fragment of the *snail2* enhancer/promoter, which allows direct imaging of NC derivatives in live embryos (J.L., M.P. and S.W., unpublished). We injected individual

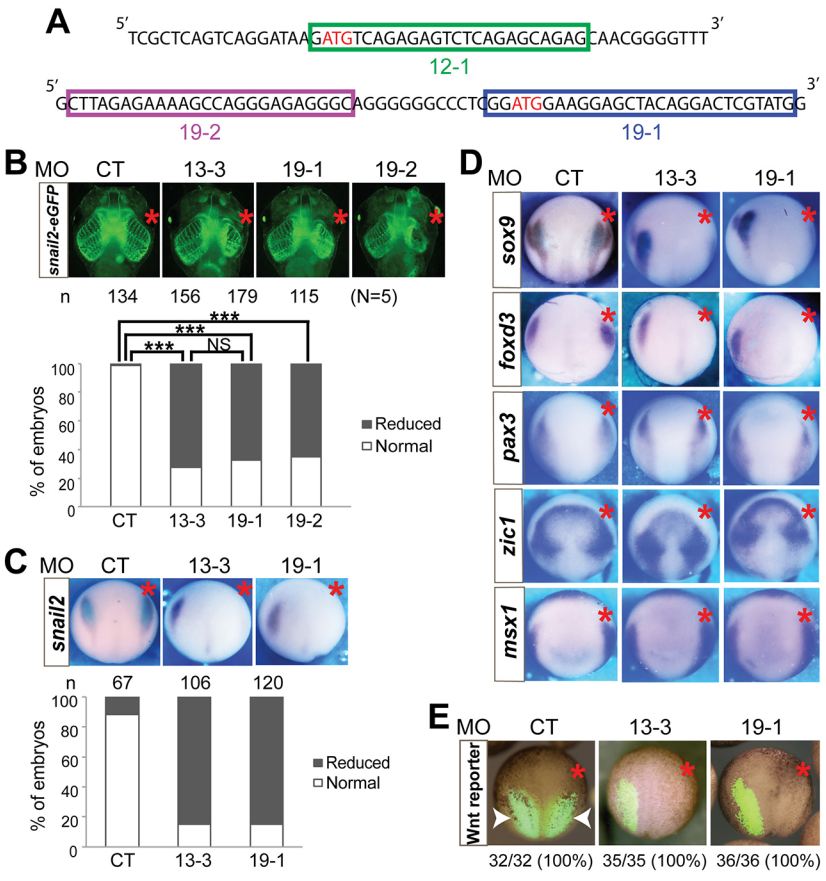

Fig. 1. Knockdown of ADAM13 or ADAM19 inhibits Wnt signaling and NC specification but not NPB formation. (A) cDNA sequences of *adam12* and *adam19* showing the translation start sites (red) and targets of MOs (colored boxes). (B) Knockdown (KD) of ADAM13 or ADAM19 inhibits head cartilage formation. Transgenic *X. tropicalis snail2-eGFP* embryos were injected in one anterodorsal (D1) blastomere at the eight-cell stage with the indicated MO (1.5 ng each) cultured to stage ∼46 and imaged for eGFP expression. One representative embryo of each injected group (ventral view) is shown in the upper panels and the results of five independent experiments are shown in the lower panel. (C,D) Effects of ADAM13 or ADAM19 KD on NC and NPB marker expression. Wild-type embryos were injected in one blastomere at the two-cell stage with the indicated MO (6 ng each) and cultured to stage ∼12.5. Embryos were processed for *in situ* hybridization for the indicated genes. (E) KD of ADAM13 or ADAM19 inhibits endogenous Wnt signaling. Transgenic Wnt reporter embryos were injected as in C,D, cultured to stage ∼12.5 and imaged for eGFP expression. White arrowheads indicate the Wnt signal at the NPB. Embryos in C-E are shown in dorsal view, with anterior at the top. Red asterisks indicate the injected side. CT, control MO; *n*, number of embryos scored; N, number of independent experiments performed; ***P<0.001; NS, not significant.

Development (2018) 145, dev158154. doi:10.1242/dev.158154

MOs to target the anterodorsal region of the *snail2* reporter embryos, and raised these embryos ('morphants') to tadpole stages. Although ADAM12 morphants displayed no apparent phenotype (data not shown), injection of either ADAM19 MO (MO 19-1 or 19-2) led to reduction in head cartilage structure on the injected side, a phenotype similar to that caused by ADAM13 MOs (MOs 13-3 and 13-1; Fig. 1B) (Wei et al., 2010b). Because the head cartilage structures are NC derivatives and ADAM13 is known to induce the NC, we tested whether loss of ADAM19 also affects NC induction. Indeed, *in situ* hybridization results show that KD of either ADAM13 or ADAM19 drastically reduced the NC marker/specifier *snail2* at stage ∼12.5 (Fig. 1C), when NC specification has just started, suggesting that both ADAMs are essential for NC induction.

Another phenotype caused by ADAM13 KD is the impaired eye structures (Wei et al., 2012), which was also manifested in ADAM19 morphants (Fig. S2A). Examination of the eye-field markers *pax6* and *rx1* reveals that both markers were downregulated by stage ∼12.5 (Fig. S2B,C) (Wei et al., 2012), indicating that depletion of either ADAM13 or 19 interferes with early eye field induction. Therefore, KD of ADAM19 phenocopies ADAM13 loss of function by inhibiting the induction of both the NC and eye field.

Both ADAM13 and ADAM19 are required for Wnt signaling and NC specification but not for NPB formation

Because NC induction occurs in two steps, the initial formation of the NPB and the subsequent specification of NC lineage, we asked which step(s) are controlled by ADAM13 and ADAM19? In addition to *snail2*, *sox9* and *foxd3*, two other NC markers/specifiers, were both downregulated at stage ∼12.5 by KD of ADAM13 or ADAM19; however, little or no effect was detected for NPB markers/specifiers *pax3*, *zic1* or *msx1* (Fig. 1D). We conclude from these results that both ADAM13 and ADAM19 are required for NC specification but not for earlier NPB formation.

The pivotal role of ADAM13 in NC specification has been attributed to its ability to regulate the activation of canonical Wnt signaling, as KD of ADAM13 inhibits Wnt8-induced axis duplication, and restoration of Wnt signaling rescues the NC defects caused by ADAM13 KD (Wei et al., 2010b). Wnt is thought to be essential for both the earlier NPB formation and the subsequent NC specification (Abu-Elmagd et al., 2006; Simões-Costa and Bronner, 2015; Stuhlmiller and García-Castro, 2012). The inhibition of NC specification but not NPB formation by KD of ADAM13 or ADAM19 suggests that these ADAM proteins may be required for Wnt activation at the established NPB to specify the NC lineage. To test this hypothesis, we took advantage of another transgenic *X. tropicalis* eGFP reporter line, which has been shown to faithfully report the endogenous Wnt activity (Tran et al., 2010). At stage ∼12.5, we detected strong eGFP signal at the NPB in the Wnt reporter embryos (Fig. 1E, white arrowheads), confirming that Wnt signaling is highly active at the NPB. Although Wnt signaling is also required for NPB formation, this earlier step (at stage ∼10.5) occurs roughly 3.5 h prior to stage ∼12.5 in *X. tropicalis* embryos at our experimental temperature (22°C). Because the destabilized eGFP protein used in the Wnt reporter line has a half-life of around 2 h (Tran et al., 2010), it is unlikely that the strong Wnt signal we observed here was the remnant of NPB formation. Depletion of ADAM13 drastically downregulated eGFP expression at the NPB in all injected embryos, and this effect was again mimicked by ADAM19 KD (Fig. 1E). Thus, both ADAM13 and ADAM19 are required in the right place and at the right time for Wnt activation to specify the NC lineage.

Function of ADAM19 in NC specification is independent of its protease activity

The striking similarity between the loss-of-function phenotypes of ADAM13 and ADAM19 implies a connection between the *in vivo* roles of these two metalloproteinases. Because ADAM19 is one of the closest paralogs of ADAM13 (Bahudhanapati et al., 2015; Wei et al., 2010a), the simplest explanation is that these two ADAMs have redundant functions. To examine whether this is the case, we first compared the *in vivo* roles of the protease activities of ADAM13 and ADAM19.

As shown in Fig. 2A, ectopic expression of wild-type ADAM13 caused anterior expansion of the expression domains of *snail2* and *sox9*, effects that are similar to those caused by ectopically expressed β-catenin or a dominant-negative EphB receptor (Hong et al., 2008; Li et al., 2009; Wei et al., 2010b). These results provide further support for our model that ADAM13 induces the NC by inhibiting forward ephrin B signaling and promoting Wnt signaling (Wei et al., 2010b). Conversely, overexpression of the protease-dead E340A mutant of ADAM13 greatly reduced both *snail2* and *sox9* (Fig. 2A), suggesting that this mutant dominant-negatively inhibited NC specification. The dominant-negative effect of the E/A mutants has been reported for several ADAMs, including ADAM13 (Alfandari et al., 2001), and is presumably caused by the abilities of the mutants to bind and sequester substrates from the endogenous ADAM proteases. The expansion and inhibition of the NC caused by wild-type ADAM13 and the E340A mutant, respectively, confirm the importance of ADAM13 protease activity in NC specification. Surprisingly, ectopic expression of wild-type ADAM19, as well as the protease-dead E345A mutant, slightly expanded the expression domains of *snail2* and *sox9* (Fig. 2A), indicating that ADAM19 may function independently of its protease activity. We further tested whether the E345A mutant can rescue the NC specification defects caused by ADAM19 KD. Indeed, co-injection of the mRNA encoding either the wild-type ADAM19 or the E345 mutant with MO 19-1 rescued the reduction in *snail2* and *sox9* expression (Fig. 2B). This is in stark contrast to our previous observations that wild-type ADAM13, but not the E340A mutant, rescued the NC-specification defects caused by ADAM13 KD (Wei et al., 2010b). These results indicate a fundamental difference in the mechanism of action for the two ADAMs: unlike ADAM13, the protease activity of ADAM19 is dispensable for its function in NC specification.

ADAM19 non-proteolytically regulates ADAM13 protein levels *in vivo*

The ability of wild-type ADAM19 and the E345A mutant to rescue the NC specification phenotypes caused by MO 19-1 confirms that these phenotypes are specific for ADAM19 KD. To further examine the efficacy and specificity of ADAM13 and 19 MOs, we assessed the abilities of these MOs to inhibit the translation of corresponding mRNA targets, as well as their closest paralogs. Western blot analyses show that each MO knocked down its target protein (Fig. 3A, lanes 4, 11 and 12). However, both MOs 19-1 and 19-2, two ADAM19 MOs with no overlap in their sequence (Fig. 1A), drastically downregulated the exogenously expressed ADAM13 (Fig. 3A, lanes 5 and 6). By contrast, the ADAM12 MO (MO 12-1) did not have a significant effect on ADAM13 (lane 3), and neither MO 12-1 nor 13-1 downregulated ADAM19 (lanes 9 and 10). Moreover, ectopically expressed ADAM10 and ADAM12 were also unaffected by MO 19-1 (data not shown), suggesting that the loss of ADAM13 caused by MO 19-1 or 19-2 was specific. Western blot analyses using an anti-ADAM13 antibody further show that

Development (2018) 145, dev158154. doi:10.1242/dev.158154

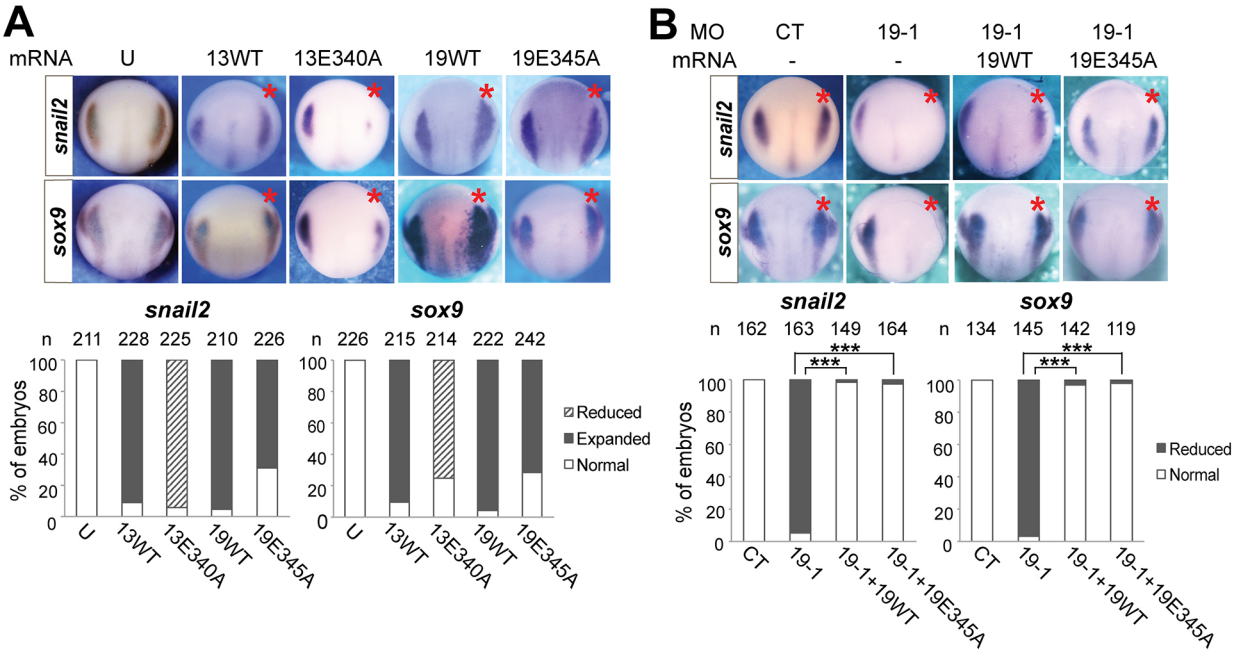

Fig. 2. ADAM13 and ADAM19 function in NC specification through different mechanisms. Wild-type embryos were injected into one blastomere at the two-cell stage with the indicated MO (6 ng each) and mRNA (100 pg each), cultured to stage ∼12.5 and processed for *in situ* hybridization for the indicated genes. (A) Effects of ectopically expressed ADAM13 and ADAM19 variants on NC markers. (B) Both wild-type ADAM19 and the protease-dead E/A mutant rescue the NC specification defects caused by ADAM19 KD. Rescue constructs were generated as described in the Materials and Methods. All embryos are shown in dorsal view, with anterior at the top and a red asterisk denoting the injected side. U, uninjected; WT, wild type. ***P<0.001.

whole-embryo injections of MO 19-1 or 19-2 resulted in over 60% reduction of endogenous ADAM13 in stage ∼12.5 *X. tropicalis* embryos; a similar effect was observed in *X. laevis* embryos (Fig. 3B and data not shown). It is unlikely that the loss of endogenous and exogenous ADAM13 in embryos injected with MO 19-1 or 19-2 was caused by off-target effects, as the transcripts of *adam13* and *adam19* do not share any significant sequence similarity despite the moderate homology between the two proteins (∼43% identities); we were also unable to detect any potential binding sites for either MO 19-1 or 19-2 on ADAM13 mRNA. Rather, these results imply that ADAM19 somehow post-transcriptionally regulates ADAM13 levels in *Xenopus* embryos. This is further supported by our observation that exogenous ADAM19 increased the levels of co-expressed ADAM13 in *X. tropicalis* embryos (Fig. 3C). Notably, a comparable increase in ADAM13 was observed with both wild-type ADAM19 and the protease-dead E345A mutant (Fig. 3C), suggesting that the regulation of ADAM13 is independent of ADAM19 protease activity.

ADAM13 and ADAM19 colocalize in the ER and interact with each other

To further investigate the interaction between ADAM13 and ADAM19, we determined the subcellular localization of these proteins in *Xenopus* XTC cells. Owing to the low expression levels of ADAM19 in XTC cells, we overexpressed this protein. Immunocytochemistry results reveal that the exogenous ADAM19 was predominantly localized to the ER, as shown by the overlapping patterns of ADAM19 and the ER marker calnexin (Fig. 4A). Our bioinformatic analyses also suggest that there are multiple possible ER-localization signals in the cytoplasmic tail of ADAM19 (R. Neuner, PhD Thesis, University of Massachusetts-Amherst, MA, USA, 2011). The endogenous ADAM13 colocalized with the exogenous ADAM19, but there was also a significant part of ADAM13 that was found in the lamellipodia (Fig. 4B). The localization of ADAM13 to the lamellipodia is consistent with the function of this protease in cleaving cell-surface substrates, such as cadherin 11, to promote migration (McCusker et al., 2009). Similar colocalization of ADAM13 and ADAM19 was also detected in 293T cells (data not shown).

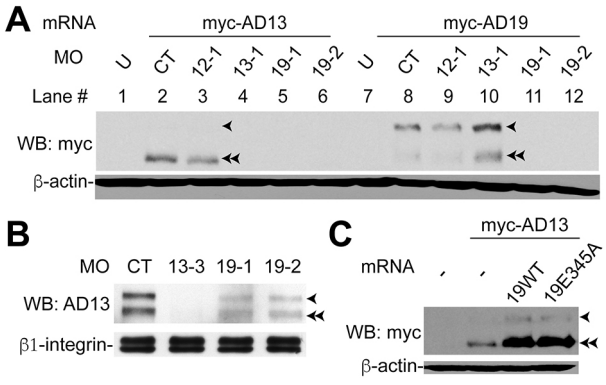

Fig. 3. ADAM19 controls ADAM13 protein levels *in vivo*. (A) Effects of various MOs on exogenously expressed ADAM13 and ADAM19. Embryos were injected in one blastomere at the two-cell stage with the indicated RNA (100 pg each) and MO (6 ng each), and cultured to stage ∼19. Whole-embryo lysates were processed for western blot (WB) for the C-terminal myc_6 tag on the ADAM constructs. (B) Effects of various MOs on endogenous ADAM13. One-cell stage embryos were injected with the indicated MO (12 ng each) and cultured to stage ∼12.5. Embryo lysates were processed for western blot for endogenous ADAM13. (C) Upregulation of exogenous ADAM13 by co-expressed ADAM19. Embryos were injected with the indicated transcripts (100 pg each; the encoded ADAM13 was myc_6-tagged and ADAM19 was HA-tagged) and cultured as in A, and lysates were processed for western blot with an anti-myc antibody. Single and double arrowheads indicate the pro- and mature forms of ADAMs, respectively.

Development (2018) 145, dev158154. doi:10.1242/dev.158154

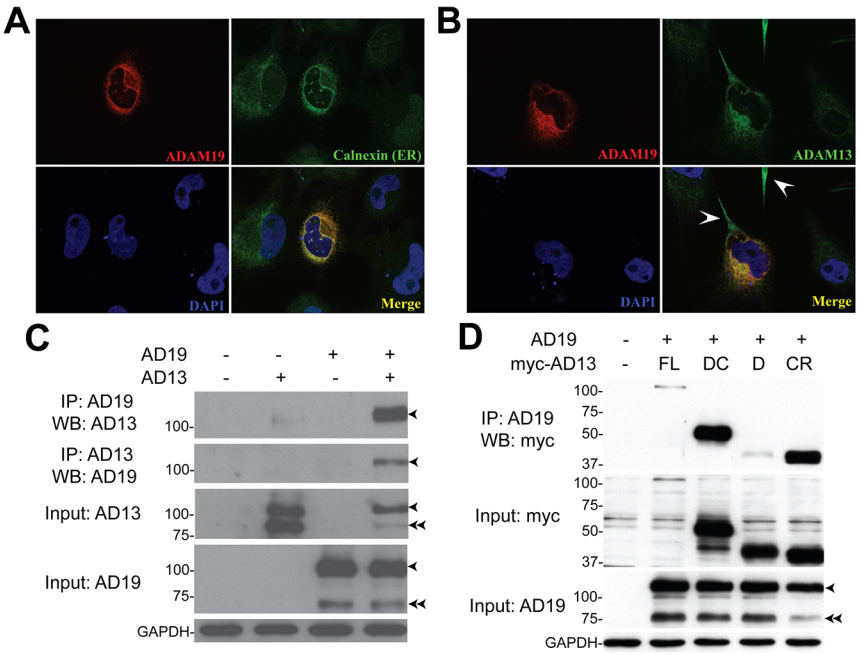

Fig. 4. ADAM19 colocalizes and interacts with ADAM13. (A,B) Colocalization of ADAM13 and ADAM19 in the ER. XTC cells were transfected with 1 µg of plasmid encoding ADAM19, and immunocytochemistry for ADAM19 (red), calnexin (green in A) and ADAM13 (green in B), as well as DAPI labeling for nuclei (blue) were carried out. Arrowheads indicate lamellipodia. (C,D) Association of ADAM19 with ADAM13. HEK293T cells were transfected with plasmids (0.5 µg each) encoding ADAM19 and untagged ADAM13 (C) or different variants of myc_6-tagged ADAM13 (D). Immunoprecipitation and western blot were carried out with the indicated antibodies. Single and double arrowheads indicate the pro- and mature forms of ADAMs, respectively. CR, cysteine-rich domain; D, disintegrin domain; DC, disintegrin and cysteine-rich domains; FL, full-length protein.

We further examined whether ADAM13 and ADAM19 physically interact with each other by overexpressing both ADAM proteins in 293T cells. Immunoprecipitation of either ADAM13 or ADAM19 pulled down the other ADAM that was co-expressed, indicating that these two ADAMs were associated with each other (Fig. 4C). To identify the domain(s) of ADAM13 that are responsible for interacting with ADAM19, we co-expressed ADAM19 with full-length ADAM13, or the disintegrin and cysteine-rich domains individually and combined, in 293T cells. Results of co-immunoprecipitation experiments show a strong association of ADAM19 with the cysteine-rich domain of ADAM13 (Fig. 4D), suggesting that this domain plays a major role in the interaction between ADAM13 and ADAM19.

ADAM19 protects ADAM13 from ubiquitin-proteasome-mediated degradation

We next asked how the interaction between ADAM13 and ADAM19 results in the increase of ADAM13 levels, as seen in Fig. 3. Because ADAM13 is known to cleave itself (Gaultier et al., 2002), it is possible that binding of ADAM19 to ADAM13 prevents the autocleavage of ADAM13. If this were the case, KD of ADAM19 should have no effect on the protease-dead E340A mutant of ADAM13. As shown in Fig. 5A, ectopic expression of wild-type ADAM13 with a C-terminal myc_6 tag gave rise to a smaller fragment (indicated by an asterisk) in addition to the pro- and mature forms of ADAM13. This fragment was not present in embryos expressing the E340A mutant, indicating that it was the C-terminal autocleavage product. Both the E340A mutant and the autocleavage product of wild-type ADAM13 were effectively downregulated by MO 19-1, arguing against the possibility that ADAM19 inhibits the autocleavage of ADAM13. By contrast, KD of ADAM13 resulted in an increase of the autocleavage product of ADAM19 (Fig. S3). Together, these data suggest that the interaction between these two ADAMs inhibits the autocleavage of ADAM19 but not ADAM13. Interestingly, MO 19-1 had little effect on the levels of an ADAM13 mutant with the cytoplasmic tail deleted (ΔC; Fig. 5A). Thus, the cytoplasmic tail of ADAM13, but not the protease activity, is crucial for the regulation by ADAM19.

We have previously found that deletion of the cytoplasmic tail results in an ∼8-fold increase in cell surface levels of *X. laevis* ADAM13 (Alfandari et al., 2001). A similar effect was observed for *X. tropicalis* ADAM13 (Fig. 5F), raising the possibility that the cytoplasmic tail may regulate the turnover of ADAM13, and that such turnover may be blocked by ADAM19. One of the most common mechanisms for membrane protein turnover is the ubiquitylation of the cytoplasmic tail, which targets the proteins for proteasome-mediated degradation (MacGurn et al., 2012). Owing to difficulties in detecting endogenously ubiquitylated ADAM13, we co-expressed HA- or myc_6-tagged ADAM13 with FLAG-tagged ubiquitin in 293T cells. Co-immunoprecipitation assays detected FLAG-tagged ubiquitin that was associated with ADAM13 (Fig. 5B,E), suggesting that ADAM13 can be ubiquitylated. To test whether ADAM13 undergoes proteasome-mediated degradation *in vivo*, we dissociated *X. tropicalis* embryos expressing ectopic ADAM13, and cultured the cells with and without the proteasome inhibitor MG132. Western blot analyses show significantly higher levels of ADAM13 upon MG132 treatment (Fig. 5C). Notably, MG132 rescued the effects of ADAM19 KD on the levels of ADAM13 (Fig. 5C), indicating that ADAM19 regulates the proteasomal degradation of ADAM13.

The C-terminal K911 residue is essential for ADAM13 turnover and regulation by ADAM19

There are 20 lysine residues in the cytoplasmic tail of *X. tropicalis* ADAM13, and our prediction using the BDM-PUB algorithm suggests that the most C-terminal K911 residue has a very high probability of being ubiquitylated (Table 1). This lysine residue is conserved in ADAM13 from fish to opossums, but not in the orthologs from higher mammals, such as mice or humans. Some other ADAMs, including the closely related ADAM12 from all animal species examined, also contain a lysine residue at the C terminus that is likely ubiquitylated (Table 1 and data not shown), suggesting a possible common mechanism of regulation. To examine the role of the K911 residue of *X. tropicalis* ADAM13, we mutated this residue to arginine. When the same amount of expression plasmid was transfected into XTC or the mammalian

Development (2018) 145, dev158154. doi:10.1242/dev.158154

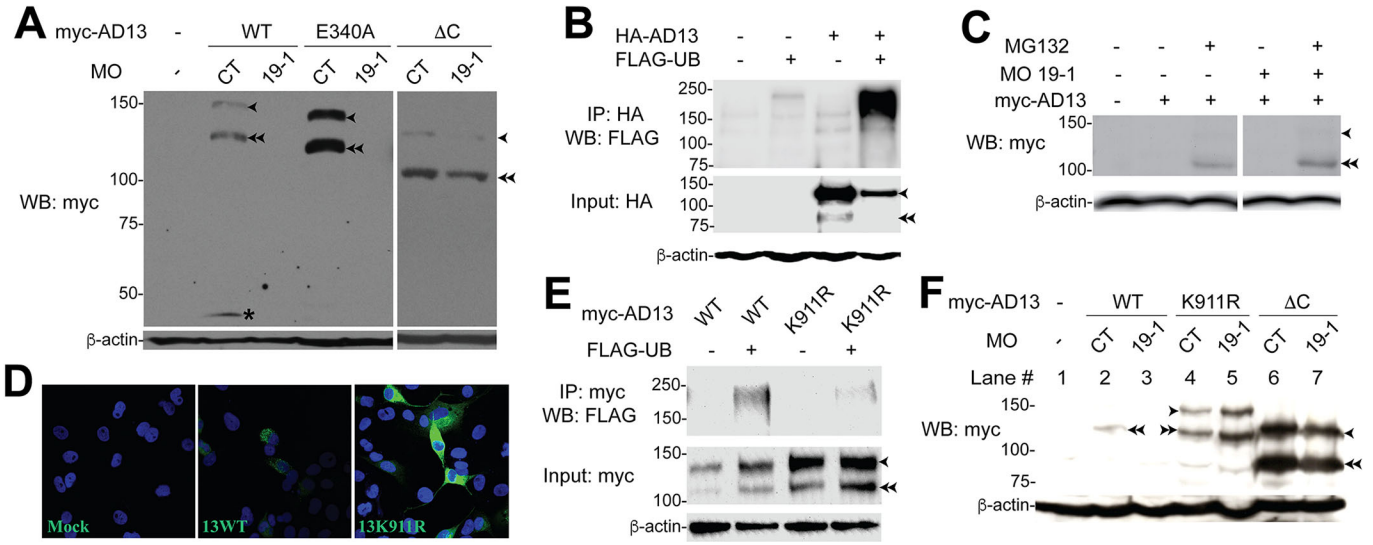

Fig. 5. The cytoplasmic K911 residue is crucial for ubiquitin-proteasome-mediated ADAM13 turnover and regulation by ADAM19. (A,F) Responses of different variants of ADAM13 to ADAM19 KD. Embryos were injected in one blastomere at the two-cell stage with the indicated RNA (100 pg each) and MO (6 ng each), and cultured to stage ~19. Whole-embryo lysates were processed for western blot for the C-terminal myc_6 tag on the ADAM constructs. A shorter exposure was performed for the ΔC mutant in B,E. Ubiquitylation of wild-type ADAM13 and the K911R mutant. HEK293T cells were transfected to express the FLAG-tagged ubiquitin with and without HA-tagged ADAM13 (B), or myc_6-tagged wild-type ADAM13 or the K911R mutant (E). Immunoprecipitation and western blot were carried out with the indicated antibodies. (C) MG132 protects ADAM13 and rescues the effect of ADAM19 KD on ADAM13. Embryos were injected, dissociated and cultured in the absence or presence of MG132. Cell lysates were processed for western blot. (D) XTC cells were transfected with 0.5 µg of plasmids encoding myc_6-tagged wild-type ADAM13 or the K911R mutant. Immunocytochemistry for myc (green) and DAPI labeling for nuclei (blue) with images taken in green and blue channels merged. Single and double arrowheads indicate the pro- and mature forms of ADAM13, respectively; asterisk denotes the autocleavage product. UB, ubiquitin.

293T or 3T3 cells, the K911R mutant was expressed consistently at higher levels than wild-type ADAM13 (Fig. 5D and data not shown). Importantly, when compared with wild-type ADAM13, the K911R mutant had reduced ubiquitylation when co-expressed with FLAG-tagged ubiquitin in 293T cells (Fig. 5E).

To assess the effects of ubiquitin on ADAM13 function in NC specification, we injected the same amount of transcripts encoding different variants of ADAM13, with and without the plasmid encoding ubiquitin, into *X. tropicalis* embryos. Similar to wild-type ADAM13, both the ectopically expressed K911R and ΔC mutants were able to induce an expansion of the *sox9* expression domain. Although co-expressed ubiquitin completely inhibited the expansion of *sox9* expression induced by wild-type ADAM13 and even caused a reduction of endogenous *sox9*, the effect was much weaker on the K911R mutant and nearly nonexistent on the ΔC mutant (Fig. S4). Finally, we determined the responses of different ADAM13 variants to ADAM19 MO *in vivo*. As shown in Fig. 5F, both the K911R and ΔC mutants were expressed at higher levels than wild-type ADAM13; unlike wild-type ADAM13, neither the K911R nor the ΔC mutant was reduced upon ADAM19 KD. Therefore, the K911 residue of ADAM13 is likely ubiquitylated and is essential for the regulation by ADAM19.

Table 1. Prediction of ubiquitylation sites in ADAMs

Protein	C-terminal sequence	Score
Zebrafish ADAM13	935 PLIVPAVFRK 944	3.7
X. tropicalis ADAM13	902 AAAAAFLQRK 911	5.3
Anolis ADAM13	956 VQTSSFPFKK 965	4.5
Chick ADAM13	938 VQSTSFPLKK 947	4.4
Opossum ADAM13	934 PGRGSLTLKK 943	4.8
Mouse ADAM12	894 PRPSHNAYIK 903	4.3
Mouse ADAM6	745 RSWQEQAKDK 754	4.6

The C-terminal 10 residues of ADAMs from indicated species are aligned, and the lysine (K) residue at or near the C terminus is underlined. Scores indicate the probabilities of this lysine residue being ubiquitylated, as predicted by the BDM-PUB algorithm (http://bdmpub.biocuckoo.org). Scores above threshold (0.3 or higher) suggest high probability of ubiquitylation.

Stabilized ADAM13 mutants rescue the NC specification defects caused by ADAM19 KD

The requirement of ADAM19 for maintaining the protein levels of ADAM13, along with the similarity between the phenotypes of ADAM13 and ADAM19 KDs, strongly implies that ADAM19 may function through regulation of ADAM13. To test this hypothesis, we evaluated the abilities of both ADAMs to rescue each other's KD phenotypes. The ΔC and K911R mutants, but not wild-type ADAM13 that was depleted upon ADAM19 KD, effectively rescued the NC specification phenotypes caused by ADAM19 KD, as shown by *in situ* hybridization for *snail2* and *sox9* (Fig. 6A and Fig. S5A). We also noticed that there was ectopic *snail2* expression in embryos injected with either the ΔC or the K911R mutant, even in the presence of ADAM19 MO (Fig. S5A), suggesting that both mutants are sufficient to induce *snail2* expression outside of the NC territory independently of ADAM19 (to be further investigated below). To rule out the possibility that the myc_6 tag interferes with the biochemical properties of ADAM13, we generated constructs encoding untagged ADAM13 variants. The untagged ΔC and K911R mutants were indistinguishable from their myc_6-tagged counterparts in rescuing the NC specification defects caused by MO 19-1 and in inducing ectopic *snail2* (Fig. S5B), confirming that the myc_6 tag does not affect ADAM13 function. By contrast, neither wild-type ADAM19 nor the E/A mutant was able to rescue the reduced *sox9* expression caused by ADAM13 MO (Fig. 6B). Taken together, these data indicate that the *in vivo* function of ADAM19 in NC specification is dependent on ADAM13, but not vice versa. We further tested whether the eye field induction defects caused by

Development (2018) 145, dev158154. doi:10.1242/dev.158154

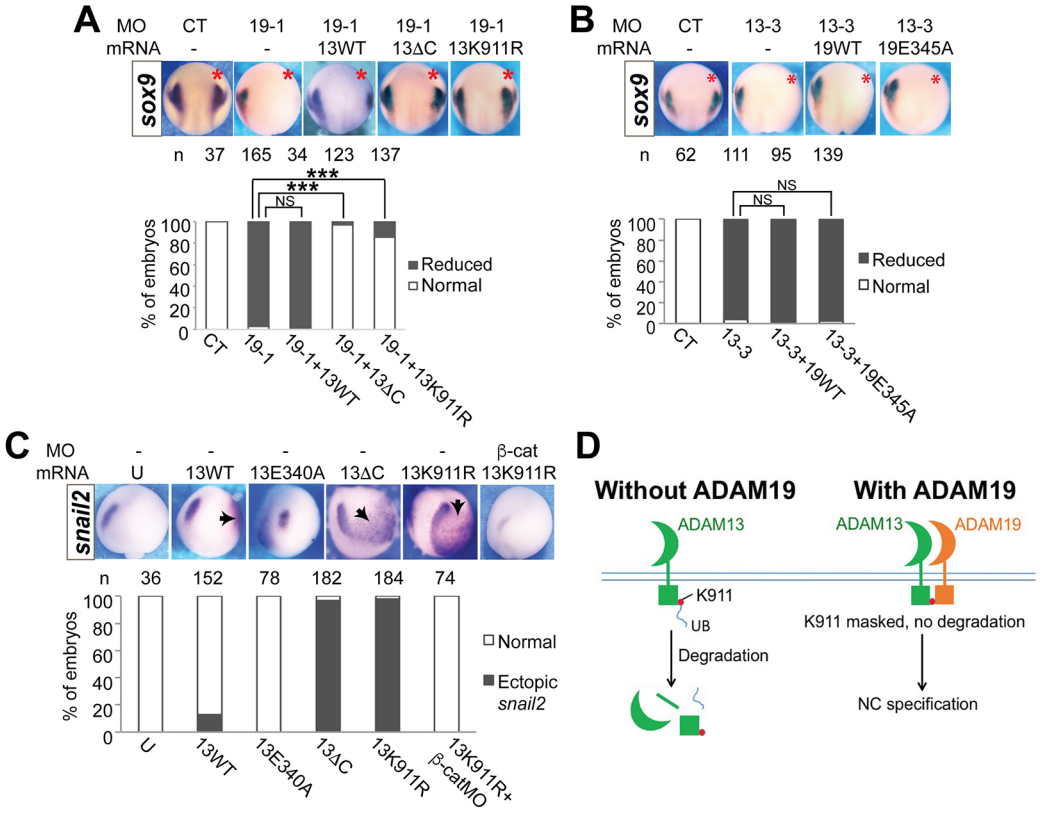

Fig. 6. The stabilized ADAM13 mutants can rescue the NC specification defects caused by ADAM19 knockdown and induce ectopic *snail2* in the ventral ectoderm. (A,B) Rescue of the reduced *sox9* expression caused by ADAM19 knockdown (KD) (A) or ADAM13 KD (B) by various transcripts. Embryos were injected into one blastomere at the two-cell stage with the indicated RNA (100 pg each) and MO (6 ng each), cultured to stage ~12.5 and processed for *in situ* hybridization for *sox9*. Embryos are shown in dorsal view, with anterior at the top and a red asterisk indicating the injected side. (C) Induction of ectopic *snail2* by different variants of ADAM13. Embryos were injected into one posterior-ventral (V2) blastomere at the eight-cell stage with the indicated RNA (50 pg each) and MO (1.5 ng each), cultured to stage ~12.5, and processed for *in situ* hybridization for *snail2*. Only the injected side is shown, with anterior at the top and dorsal to the left. Arrows indicate the ectopic *snail2* expression. (D) A model for the regulation of ADAM13 stability and NC specification by ADAM19. Crescents indicate the metalloproteinase domains of ADAMs. See Discussion for an explanation. ***P<0.001; NS, not significant.

ADAM19 KD can also be rescued by the ΔC and K911R mutants of ADAM13. Indeed, expression of the eye field markers *pax6* and *rx1* was restored when mRNA encoding either ADAM13 mutant was co-injected with MO 19-1 (Fig. S6), suggesting that ADAM19 also functions in eye-field induction by regulating ADAM13.

Ectopic expression of stabilized ADAM13 mutants induces *snail2* in the future epidermis

We have previously identified Snail2 as a major downstream target that mediates ADAM13 function in NC specification, as exogenous Snail2 rescued the NC defects caused by ADAM13 KD (Wei et al., 2010b). Our current finding that the ΔC and K911R mutants of ADAM13 can induce ectopic *snail2* in the dorsal ectoderm (Fig. S5A,B) not only validates these results, but also suggests that the ADAM13-Wnt signaling axis may partially re-specify non-NC cells to adopt some NC-like properties. To test this possibility, we injected transcripts encoding different variants of ADAM13 into the posterior-ventral region of *X. tropicalis* embryos, where the cells are destined to become epidermis and do not express detectable levels of endogenous *snail2*. As shown in Fig. 6C, a low dose of mRNA encoding wild-type ADAM13 induced weak ectopic expression of *snail2* in the ventral ectoderm, whereas the same amount of the ΔC and K911R mutant transcripts caused a robust induction. A similar induction of *snail2* expression by wild-type ADAM13 was obtained in animal cap assays using *X. laevis* embryos (Khedgikar et al., 2017). By contrast, the E/A mutant failed to induce ectopic *snail2*, and co-injecting a β-catenin MO completely abolished the *snail2*-inducing activity of the K911R mutant (Fig. 6C). These results are consistent with our previous observations that ADAM13 protease activity and downstream Wnt signaling are required for NC specification (Wei et al., 2010b). However, we were unable to detect any ectopic expression of other NC or NPB specifiers that were tested, including *sox9*, *foxd3*, *pax3*, *zic1* and *msx1*, in any of these embryos (data not shown). Thus, the ADAM13-Wnt axis is sufficient to induce *snail2* in the ventral ectoderm but not to produce a complete conversion to the NC lineage.

DISCUSSION

Many extracellular metalloproteinases, including several ADAMs, have been implicated in NC development (Christian et al., 2013). The ADAMs are key regulators of cell signaling, mainly due to their abilities to cleave signaling molecules such as ligands, receptors, agonists and antagonists. However, some ADAM proteases may function through their non-proteolytic activities in certain physiological contexts, and there are also non-proteolytic ADAMs that play important roles in development and disease (Edwards et al., 2008; Reiss and Saftig, 2009). As compared with the well-characterized functions of ADAM protease activities, little is known about the non-proteolytic roles of ADAMs *in vivo*. Here we report that *Xenopus* ADAM19 specifies the NC lineage through

Development (2018) 145, dev158154. doi:10.1242/dev.158154

non-proteolytic protection of ADAM13. To our knowledge, there is no published example of one protease protecting another *in vivo*. A possible mechanism for this novel protease-protease interaction is discussed below.

The first two testicular ADAMs, ADAMs 1 and 2, were discovered as a heterodimer that is involved in sperm-egg fusion (Blobel et al., 1992). However, the physiological consequence of this dimerization is unclear, and similar interaction has not been reported for somatic ADAMs. Instead, ADAMs 10 and 17, two somatic ADAMs, are known to interact with tetraspanins and non-proteolytic members of the Rhomboid family (iRhoms), respectively, which regulate the trafficking, stability and activity of these ADAMs (Adrain et al., 2012; Dornier et al., 2012; Haining et al., 2012; Matthews et al., 2017; McIlwain et al., 2012). The activity of *Xenopus* ADAM13 has also been shown to be regulated by other proteins, such as PACSIN2 and XFz4 (Abbruzzese et al., 2015; Cousin et al., 2000). In the current study, we observed a protective effect of ADAM19 towards ADAM13, which underlies the *in vivo* function of ADAM19 in NC specification. Our data suggest that, in the absence of ADAM19, ADAM13 is ubiquitylated at the C-terminal K911 residue and degraded through the proteasome pathway. When ADAM19 is present, it binds to the cysteine-rich domain of ADAM13 and possibly masks the K911 residue in the cytoplasmic tail of ADAM13, resulting in the stabilization of ADAM13 that subsequently specifies the NC lineage (Fig. 6D). Interestingly, although ADAM13 inhibits the autocleavage of ADAM19, ADAM19 does not seem to cleave ADAM13 or interfere with its protease activity (Fig. S3 and Fig. 5A). Therefore, the heterodimer is likely asymmetric: although the protease activity of ADAM19 may be blocked by ADAM13, ADAM13 remains free to cleave its substrates (Fig. 6D). This structural asymmetry is likely crucial for the difference in the mechanism of action for the two ADAMs in NC specification.

Most of the studies on the functions of ADAMs in early NC development have been carried out in two *Xenopus* species, *X. laevis* and *X. tropicalis* (Christian et al., 2013). Our previous work unveiled the essential roles of ADAM13 in NC induction in *X. tropicalis* embryos (Wei et al., 2010b), which is confirmed by the current study. However, KD of ADAM13 in *X. laevis* did not affect any NC markers, raising the issue of whether the function of ADAM13 in NC induction is conserved (Cousin et al., 2011). A major difference between the two frog species is that *X. tropicalis* is diploid, whereas *X. laevis* is allotetraploid (Session et al., 2016). The *X. laevis* genome contains a pseudoallelle of *adam13* (also known as *xmdc13*), which encodes a protein that is ∼88% and 87% identical to *X. laevis* and *X. tropicalis* ADAM13, respectively (Cai et al., 1998). KD of both ADAM13 and xMDC13 did result in reduction of *snail2* expression prior to NC migration in *X. laevis* embryos (D.A., unpublished), indicating that ADAM13 function in NC specification is conserved between the two frog species. Unlike *adam13*, there is only one copy of *adam19* in *X. laevis*, and KD of this gene also causes reduction of pre-migratory NC markers at stage ∼15 (Neuner et al., 2009). However, it was unclear whether this effect was caused by inhibition of induction or post-induction maintenance of the NC. Combined with the current study, these results suggest that ADAM19 is required for NC specification in both *Xenopus* species. At later stages, ADAM13 is required for NC migration through its protease activity, as well as the cytoplasmic tail, which is cleaved and translocalizes into the nucleus to regulate target gene transcription (Cousin et al., 2011). By contrast, we show here that the function of ADAM13 in NC specification is independent of its cytoplasmic tail, as the ΔC mutant can effectively rescue the early NC defects caused by ADAM19 KD and induce ectopic *snail2* (Fig. 6A,C, Fig. S5A,B). Thus, the mechanisms of action for ADAM13 in NC specification and migration appear to be different.

Previous research has implicated more than one wave of canonical Wnt signaling in NC induction. In *Xenopus* embryos, several Wnt ligands and receptors have been reported to have NC-inducing capacity, and loss-of-function studies have confirmed that at least two canonical Wnt ligands, Wnt3a and Wnt8, as well as two Wnt receptors, Xfz3 and Xfz7, are required for endogenous NC induction (Abu-Elmagd et al., 2006; Deardorff et al., 2001; Elkouby et al., 2010; Hong et al., 2008). These Wnt ligands and receptors are expressed in different regions at the time of NC induction (Abu-Elmagd et al., 2006; Steventon et al., 2009), suggesting that, instead of functioning redundantly, they may form separate waves of Wnt signaling to regulate different aspects of NC induction. Indeed, NC induction can be divided into two steps, the formation of NPB and the specification of NC lineage, both of which are thought to depend on Wnt signaling (Simões-Costa and Bronner, 2015). However, although the regulation of NPB markers/specifiers by Wnt signaling has been well studied, whether and how Wnt controls endogenous NC specification remained elusive. This is probably because NC specification immediately follows, and is difficult to be separated from, NPB formation. In particular, it was unclear whether the two steps of NC induction are controlled by the same wave of Wnt signaling or separate ones. In this study, we provide three important lines of evidence suggesting that a distinct wave of Wnt signaling, which is controlled by ADAM13 and ADAM19, is required for endogenous NC specification but not NPB formation in *X. tropicalis* embryos. First, by using a transgenic Wnt reporter line, we found that canonical Wnt signaling is highly active within the NPB at late gastrula stages (Fig. 1E). To our knowledge, this is the first direct evidence indicating that there is strong Wnt signal at the NPB during NC specification, although previous studies indicate that Wnt activity in NC explants increases between gastrula and neurula stages (Steventon et al., 2009). This spatiotemporal pattern of Wnt activity is consistent with its function in NC specification. Second, KD of either ADAM13 or ADAM19 inhibits Wnt signaling and NC specification at the NPB, but the formation of NPB itself is unaffected (Fig. 1C-E). These results differ from previous reports that Wnt inhibition causes loss of both NPB and NC markers (Li et al., 2009; Monsoro-Burq et al., 2005). Thus unlike the 'core' Wnt components that are required ubiquitously for Wnt signal activation, ADAM13 and ADAM19 are needed in only a subset of tissues, probably where the Wnt signal is cross-antagonized by ephrin B signaling. Such differential requirement allows us to separate the wave of Wnt signaling that specifies NC lineage from the one that establishes the NPB. Last, we show that ectopic expression of ADAM13 induces the NC specifier *snail2* in the ventral ectoderm in a Wnt-dependent manner (Fig. 6C). This gain-of-function phenotype provides additional evidence for the specification of NC lineage by the ADAM13-Wnt signaling axis. Among the NC specifier genes, *snail2* is the only one that is known to contain a *cis*-regulatory element that binds LEF/TCF transcription factors, and has been speculated to be the direct Wnt target during NC specification (Simões-Costa and Bronner, 2015). Interestingly, ADAM13 cannot induce ectopic expression of any of the other NC or NPB markers that were examined, suggesting that *snail2* is indeed the direct target of the ADAM13/19-Wnt axis. This is further supported by our previous finding that exogenous Snail2 can rescue the reduction of other NC markers, such as *sox9* and *twist*, caused by ADAM13 KD (Wei et al., 2010b).

Development (2018) 145, dev158154. doi:10.1242/dev.158154

The potential application of NC cells in tissue regeneration for the treatment of related birth defects or damages has drawn a great deal of research interest. Methods are being actively developed to differentiate pluripotent stem cells or reprogram non-NC lineages to generate NC cells (Kunisada et al., 2014; Zhu et al., 2016). In this study, we found that the stabilized ADAM13 mutants that can function independently of ADAM19 induce robust expression of the key NC specifier *snail2* in the ventral ectoderm; however, the lack of other NC or NPB markers/specifiers indicates an incomplete conversion to the NC lineage (Fig. 6C). By contrast, overexpression of ADAM13 on the dorsal ectoderm causes expansion of both *snail2* and other NC markers, such as *sox9* along the NPB (Fig. 2A), suggesting that additional molecules, which are normally present at the NPB, are needed to cooperate with ADAM13 to induce a complete conversion of the ventral ectoderm cells to NC lineage. Potential candidates include inhibitors of bone morphogenetic protein (BMP) signaling, such as Chordin and Noggin, because high BMP signal on the ventral side of the embryos is known to inhibit NC induction (LaBonne and Bronner-Fraser, 1998; Steventon et al., 2009). Our results also call for caution in interpreting some of the published data on ectopic NC induction, where *snail2* is used as the only marker for the NC lineage. Finally, Wnt signaling and Snail2 are known to be key regulators of the epithelial-to-mesenchymal transition (EMT) in development, wound repair and cancer. In the traditional models of EMT, Wnt and Snail2 control the downstream expression of metalloproteinases, which in turn modify cell-cell and cell-matrix adhesion through their proteolytic activities to promote cell migration and invasion (Lim and Thiery, 2012; Powell et al., 2013). Here, we show that both the proteolytic and nonproteolytic activities of ADAMs play important roles upstream to regulate Wnt signaling and *snail2* expression. It would be of interest to examine whether similar mechanisms are also involved in developmental and/or pathological EMT.

MATERIALS AND METHODS

Plasmids and antibodies

X. tropicalis cDNA clones encoding *adam12*, *adam13* and *adam19* were obtained previously (Wei et al., 2010b). Constructs encoding C-terminally myc_6- or HA-tagged wild-type ADAMs were generated by subcloning into pCS2+ vectors modified to append corresponding epitopes, and mutations were introduced using a QuikChange mutagenesis kit (Stratagene). Rescue constructs were made by introducing sense mutations downstream of the translational start codon in corresponding myc_6-tagged expression constructs. Constructs for preparing the *in situ* hybridization probes for *snail2*, *sox9*, *foxd3*, *pax3*, *zic1*, *msx1*, *pax6* and *rx1* were obtained previously (Li et al., 2011; Wei et al., 2012, 2010b). The FLAG-ubiquitin construct was a gift from Dr Carole Labonne (Northwestern University, Evanston, IL, USA). *In vitro* transcription was carried out as described previously to generate mRNA transcripts and *in situ* hybridization probes (Sive et al., 2000). Commercial primary antibodies that were used in this study include: mouse anti-myc (DSHB 9E10, 1:500), mouse anti-HA (Sigma-Aldrich H9658, 1:20,000), mouse anti-FLAG (Sigma-Aldrich F1804, 1:1000) and rabbit anti-calnexin (Enzo Life Sciences ADI-SPA-860, 1:200). The rabbit anti-ADAM13 (6615F, 1:200) and anti-ADAM19 (2C5 E1, 1:200) antibodies were generated previously (Alfandari et al., 1997; Neuner et al., 2009). Commercial secondary antibodies that were used include HRP-conjugated rabbit anti-mouse (Sigma-Aldrich A9044, 1:80,000) and goat anti-rabbit (Sigma-Aldrich A0545, 1:80,000), as well as Alexa Fluor 488 donkey anti-mouse (Jackson Laboratories 715-545-150, 1:200) and Alexa Fluor 594 donkey anti-rabbit (Jackson Laboratories 711-585-152, 1:200). For loading controls, unconjugated mouse anti-β1-integrin (DSHB 8C8, 1:10), anti-GAPDH (Millipore MAB374, 1:10,000) or HRP-conjugated mouse anti-β-actin (Sigma-Aldrich A5316, 1:5000) were used.

Animals and embryo manipulation

Wild-type *X. tropicalis* and *X. laevis* adults (male and female) were purchased from NASCO. The transgenic *X. tropicalis* Wnt reporter frogs were provided courtesy of Dr Kris Vleminckx (Flanders Institute for Biotechnology, Belgium), and the transgenic *X. tropicalis snail2-eGFP* line was generated as described elsewhere (J.L., M.P. and S.W., unpublished). Methods involving live animals were carried out in accordance with the guidelines and regulations approved and enforced by the Institutional Animal Care and Use Committees at West Virginia University, University of Delaware and University of Massachusetts at Amherst. Morpholino oligos were designed and synthesized by Gene Tools. Embryo preparation, injection and culturing were carried out as described previously (Wei et al., 2010b). Briefly, embryos were obtained by natural mating and injections were carried out to target specific blastomeres (Huang et al., 1998) using a PLI-100A microinjector (Harvard Apparatus). Alexa Fluor 555 or 488 dextran (Invitrogen) was co-injected as a lineage tracer. Embryos were cultured in 0.1× MBS to desired stages, and injected embryos were sorted according to the injected side using a Zeiss Axiozoom.v16 epifluorescence microscope. Embryo lysates were prepared as described below for cell lysates. For embryo dissociation, *X. tropicalis* embryos were injected in both blastomeres at the two-cell stage and cultured to stage ∼12.5. The embryos were placed in 1.5 ml centrifuge tubes with 0.1× MBS and 100 µM MG132 (or DMSO as control). The embryos were then dissociated using a 28 gauge 1 ml syringe (Exel) and incubated in 0.1× MBS and 100 µM MG132 or DMSO at 23°C for 5 h.

Cell culture and transfection

HEK293T cells were purchased from ATCC and cultured in DMEM (ATCC) supplemented with 10% fetal bovine serum (FBS; Gibco) at 37°C with 5% CO_2. XTC cells (Pudney et al., 1973) were cultured in L-15 medium (GE Life Sciences) supplemented with 10% FBS and 1 mM sodium pyruvate at 23°C. Both cell lines were recently authenticated and tested for contamination. Cells were transfected using Lipofectamine 3000 (Invitrogen) at 50-70% confluency, and allowed to grow for another 24-48 h. For MG132 treatment, cells were cultured in the presence of 40 µM MG132 for 24 h before being harvested. To prepare whole-cell lysates, cells were lysed in ice-cold lysis buffer [20 mM Tris-HCl (pH 7.6), 100 mM NaCl, 1% Triton X-100, 50 mM NaF, 10 mM $Na_4P_2O_7$, 1 mM PMSF and 5 mM EDTA] supplemented with protease inhibitor cocktail (Sigma-Aldrich) and 10 mM *o*-phenanthroline, and centrifuged for 20 min at 12,000 ***g*** at 4°C. Supernatants were processed for SDS-PAGE and blotted with corresponding antibodies.

In situ hybridization and immunocytochemistry

Embryos were fixed at desired stages, and *in situ* hybridization was carried out as described (Sive et al., 2000). For immunocytochemistry, cells were cultured and transfected on glass coverslips (Fisher Scientific), and fixed with 1:1 methanol/acetone at −20°C for 10 min. The cells were then rehydrated with 1× PBS for 10 min, blocked with 1% bovine serum albumin (Sigma-Aldrich) for 1 h at room temperature, and incubated with the primary antibody at 4°C overnight. After being washed with PBS containing 0.5% Tween-20, the cells were subsequently incubated with Alexa Fluor-conjugated secondary antibody for 1 h at room temperature, and labeled with DAPI (Sigma-Aldrich) to identify cell nuclei. Images were captured with a Zeiss 780 multiphoton confocal microscope.

Western blot and immunoprecipitation

Detection of western blots was carried out using HRP-conjugated secondary antibodies and chemiluminescence substrates (GE Healthcare). Membranes were stripped and reblotted for β-actin, β1-integrin or GAPDH as a loading control. For immunoprecipitation, cells were lysed with 20 mM Tris-HCl, (pH 7.6), 167 mM NaCl, 1% NP-40 and protease inhibitor cocktail (Sigma-Aldrich) at 4°C for 30 min. The lysates were then centrifuged for 20 min at 12,000 ***g*** at 4°C. Supernatants were collected and incubated with 2-10 µg of antibody with rotation at 4°C overnight. Protein G PLUS-Agarose beads (Santa Cruz) were added to the mixture and rotated for 1 h at 4°C. Beads were then washed five times with ice-cold PBS. The bound proteins were dissociated by incubating with SDS-PAGE loading buffer at 50°C for

Development (2018) 145, dev158154. doi:10.1242/dev.158154

10 min and then 100°C for 10 min, and subsequently subjected to western blot analysis.

Phenotype scoring and statistics

For craniofacial phenotypes, injected *snail2-eGFP* embryos were allowed to develop to stage ∼46 and scored for defects in head cartilage structures. For eye phenotypes, injected wild-type embryos were allowed to develop to stage ∼38 and scored for defects in eye structures. Embryos were scored blinded as individuals selected randomly from the different treatment groups, by comparing the injected side with the uninjected side of the same embryos. The percentages of normal and reduced phenotypes were calculated for injected embryos obtained from multiple independent experiments, and Chi-squared tests were performed to compare the phenotypes in different treatment groups. Images of head cartilages (eGFP) or eyes (bright field) were taken with a Zeiss Axiozoom.v16 epifluorescence microscope. See also Wei et al. (2010b) and Fig. S1D for more examples and explanation of cartilage and eye phenotypes.

Acknowledgements

We thank Dr Kris Vleminckx for providing the transgenic Wnt reporter frogs, and Dr Carole Labonne for the FLAG-ubiquitin construct.

Competing interests

The authors declare no competing or financial interests.

Author contributions

Conceptualization: J.L., M.P., D.A., S.W.; Methodology: J.L., M.P., D.A., S.W.; Formal analysis: J.L., M.P., R.N., H.B., L.C., K.M., L.C.B., D.A., S.W.; Investigation: J.L., M.P., R.N., H.B., L.C., K.M., L.C.B., D.A., S.W.; Data curation: J.L., M.P., R.N., H.B., L.C., K.M., D.A., S.W.; Writing - original draft: S.W.; Writing - review & editing: M.P., L.C., D.A., S.W.; Supervision: S.W.; Project administration: S.W.; Funding acquisition: D.A., S.W.

Funding

This work was supported by the National Institutes of Health (GM114105, GM094793, GM104316, DE022813 and DE016289) and the March of Dimes Foundation (1-FY10-399). Deposited in PMC for release after 12 months.

Supplementary information

Supplementary information available online at
http://dev.biologists.org/lookup/doi/10.1242/dev.158154.supplemental

References

Abbruzzese, G., Gorny, A.-K., Kaufmann, L. T., Cousin, H., Kleino, I., Steinbeisser, H. and Alfandari, D. (2015). The Wnt receptor Frizzled-4 modulates ADAM13 metalloprotease activity. *J. Cell Sci.* **128**, 1139-1149.

Abu-Elmagd, M., Garcia-Morales, C. and Wheeler, G. N. (2006). Frizzled7 mediates canonical Wnt signaling in neural crest induction. *Dev. Biol.* **298**, 285-298.

Adrain, C., Zettl, M., Christova, Y., Taylor, N. and Freeman, M. (2012). Tumor necrosis factor signaling requires iRhom2 to promote trafficking and activation of TACE. *Science* **335**, 225-228.

Alfandari, D., Cousin, H., Gaultier, A., Smith, K., White, J. M., Darribère, T. and DeSimone, D. W. (2001). Xenopus ADAM 13 is a metalloprotease required for cranial neural crest-cell migration. *Curr. Biol.* **11**, 918-930.

Alfandari, D., Wolfsberg, T. G., White, J. M. and DeSimone, D. W. (1997). ADAM 13: a novel ADAM expressed in somitic mesoderm and neural crest cells during Xenopus laevis development. *Dev. Biol.* **182**, 314-330.

Bahudhanapati, H., Bhattacharya, S. and Wei, S. (2015). Evolution of vertebrate adam genes; duplication of testicular adams from ancient adam9/9-like loci. *PLoS ONE* **10**, e0136281.

Blobel, C. P., Wolfsberg, T. G., Turck, C. W., Myles, D. G., Primakoff, P. and White, J. M. (1992). A potential fusion peptide and an integrin ligand domain in a protein active in sperm-egg fusion. *Nature* **356**, 248-252.

Bronner, M. E. and Simões-Costa, M. (2016). The neural crest migrating into the twenty-first century. *Curr. Top. Dev. Biol.* **116**, 115-134.

Cai, H., Krätzschmar, J., Alfandari, D., Hunnicutt, G. and Blobel, C. P. (1998). Neural crest-specific and general expression of distinct metalloprotease-disintegrins in early Xenopus laevis development. *Dev. Biol.* **204**, 508-524.

Christian, L., Bahudhanapati, H. and Wei, S. (2013). Extracellular metalloproteinases in neural crest development and craniofacial morphogenesis. *Crit. Rev. Biochem. Mol. Biol.* **48**, 544-560.

Cousin, H., Gaultier, A., Bleux, C., Darribère, T. and Alfandari, D. (2000). PACSIN2 is a regulator of the metalloprotease/disintegrin ADAM13. *Dev. Biol.* **227**, 197-210.

Cousin, H., Abbruzzese, G., Kerdavid, E., Gaultier, A. and Alfandari, D. (2011). Translocation of the cytoplasmic domain of ADAM13 to the nucleus is essential for Calpain8-a expression and cranial neural crest cell migration. *Dev. Cell* **20**, 256-263.

Deardorff, M. A., Tan, C., Saint-Jeannet, J. P. and Klein, P. S. (2001). A role for frizzled 3 in neural crest development. *Development* **128**, 3655-3663.

Dornier, E., Coumailleau, F., Ottavi, J.-F., Moretti, J., Boucheix, C., Mauduit, P., Schweisguth, F. and Rubinstein, E. (2012). TspanC8 tetraspanins regulate ADAM10/Kuzbanian trafficking and promote Notch activation in flies and mammals. *J. Cell Biol.* **199**, 481-496.

Edwards, D. R., Handsley, M. M. and Pennington, C. J. (2008). The ADAM metalloproteinases. *Mol. Aspects Med.* **29**, 258-289.

Elkouby, Y. M., Elias, S., Casey, E. S., Blythe, S. A., Tsabar, N., Klein, P. S., Root, H., Liu, K. J. and Frank, D. (2010). Mesodermal Wnt signaling organizes the neural plate via Meis3. *Development* **137**, 1531-1541.

Gaultier, A., Cousin, H., Darribere, T. and Alfandari, D. (2002). ADAM13 disintegrin and cysteine-rich domains bind to the second heparin-binding domain of fibronectin. *J. Biol. Chem.* **277**, 23336-23344.

Haining, E. J., Yang, J., Bailey, R. L., Khan, K., Collier, R., Tsai, S., Watson, S. P., Frampton, J., Garcia, P. and Tomlinson, M. G. (2012). The TspanC8 subgroup of tetraspanins interacts with A disintegrin and metalloprotease 10 (ADAM10) and regulates its maturation and cell surface expression. *J. Biol. Chem.* **287**, 39753-39765.

Hong, C.-S., Park, B.-Y. and Saint-Jeannet, J.-P. (2008). Fgf8a induces neural crest indirectly through the activation of Wnt8 in the paraxial mesoderm. *Development* **135**, 3903-3910.

Huang, S., Johnson, K. E. and Wang, H. Z. (1998). Blastomeres show differential fate changes in 8-cell Xenopus laevis embryos that are rotated 90 degrees before first cleavage. *Dev. Growth Differ.* **40**, 189-198.

Khedgikar, V., Abbruzzese, G., Mathavan, K., Szydlo, H., Cousin, H. Alfandari, D. (2017). Dual control of pcdh8l/PCNS expression and function in Xenopus laevis neural crest cells by adam13/33 via the transcription factors tfap2α and arid3a. *eLife* **6**, e26898.

Kunisada, T., Tezulka, K.-I., Aoki, H. and Motohashi, T. (2014). The stemness of neural crest cells and their derivatives. *Birth Defects Res. C Embryo Today* **102**, 251-262.

LaBonne, C. and Bronner-Fraser, M. (1998). Neural crest induction in Xenopus: evidence for a two-signal model. *Development* **125**, 2403-2414.

Li, B., Kuriyama, S., Moreno, M. and Mayor, R. (2009). The posteriorizing gene Gbx2 is a direct target of Wnt signalling and the earliest factor in neural crest induction. *Development* **136**, 3267-3278.

Li, J., Shi, Y., Sun, J., Zhang, Y. and Mao, B. (2011). Xenopus reduced folate carrier regulates neural crest development epigenetically. *PLoS ONE* **6**, e27198.

Lim, J. and Thiery, J. P. (2012). Epithelial-mesenchymal transitions: insights from development. *Development* **139**, 3471-3486.

MacGurn, J. A., Hsu, P. C. and Emr, S. D. (2012). Ubiquitin and membrane protein turnover: from cradle to grave. *Annu. Rev. Biochem.* **81**, 231-259.

Matthews, A. L., Noy, P. J., Reyat, J. S. and Tomlinson, M. G. (2017). Regulation of A disintegrin and metalloproteinase (ADAM) family sheddases ADAM10 and ADAM17: The emerging role of tetraspanins and rhomboids. *Platelets* **28**, 333-341.

Mayor, R. and Theveneau, E. (2013). The neural crest. *Development* **140**, 2247-2251.

McCusker, C., Cousin, H., Neuner, R. and Alfandari, D. (2009). Extracellular cleavage of cadherin-11 by ADAM metalloproteases is essential for Xenopus cranial neural crest cell migration. *Mol. Biol. Cell* **20**, 78-89.

McIlwain, D. R., Lang, P. A., Maretzky, T., Hamada, K., Ohishi, K., Maney, S. K., Berger, T., Murthy, A., Duncan, G., Xu, H. C. et al. (2012). iRhom2 regulation of TACE controls TNF-mediated protection against Listeria and responses to LPS. *Science* **335**, 229-232.

Milet, C., Maczkowiak, F., Roche, D. D. and Monsoro-Burq, A. H. (2013). Pax3 and Zic1 drive induction and differentiation of multipotent, migratory, and functional neural crest in Xenopus embryos. *Proc. Natl. Acad. Sci. USA* **110**, 5528-5533.

Monsoro-Burq, A.-H., Wang, E. and Harland, R. (2005). Msx1 and Pax3 cooperate to mediate FGF8 and WNT signals during Xenopus neural crest induction. *Dev. Cell* **8**, 167-178.

Neuner, R., Cousin, H., McCusker, C., Coyne, M. and Alfandari, D. (2009). Xenopus ADAM19 is involved in neural, neural crest and muscle development. *Mech. Dev.* **126**, 240-255.

Powell, D. R., Blasky, A. J., Britt, S. G. and Artinger, K. B. (2013). Riding the crest of the wave: parallels between the neural crest and cancer in epithelial-to-mesenchymal transition and migration. *Wiley Interdiscip. Rev. Syst. Biol. Med.* **5**, 511-522.

Pudney, M., Varma, M. G. and Leake, C. J. (1973). Establishment of a cell line (XTC-2) from the South African clawed toad, Xenopus laevis. *Experientia* **29**, 466-467.

Reiss, K. and Saftig, P. (2009). The “a disintegrin and metalloprotease” (ADAM) family of sheddases: physiological and cellular functions. *Semin. Cell Dev. Biol.* **20**, 126-137.
Sato, T., Sasai, N. and Sasai, Y. (2005). Neural crest determination by co-activation of Pax3 and Zic1 genes in Xenopus ectoderm. *Development* **132**, 2355-2363.
Session, A. M., Uno, Y., Kwon, T., Chapman, J. A., Toyoda, A., Takahashi, S., Fukui, A., Hikosaka, A., Suzuki, A., Kondo, M. et al. (2016). Genome evolution in the allotetraploid frog Xenopus laevis. *Nature* **538**, 336-343.
Simões-Costa, M. and Bronner, M. E. (2015). Establishing neural crest identity: a gene regulatory recipe. *Development* **142**, 242-257.
Sive, H. L., Grainger, R. M., and Harland, R. M. (2000). *Early Development of Xenopus Laevis. A Laboratory Manual*. Cold Spring Harbor, NY: Cold Spring Harbor Laboratory Press.
Steventon, B., Araya, C., Linker, C., Kuriyama, S. and Mayor, R. (2009). Differential requirements of BMP and Wnt signalling during gastrulation and neurulation define two steps in neural crest induction. *Development* **136**, 771-779.
Stuhlmiller, T. J. and García-Castro, M. I. (2012). Current perspectives of the signaling pathways directing neural crest induction. *Cell. Mol. Life Sci.* **69**, 3715-3737.
Tran, H. T., Sekkali, B., Van Imschoot, G., Janssens, S. and Vleminckx, K. (2010). Wnt/beta-catenin signaling is involved in the induction and maintenance of primitive hematopoiesis in the vertebrate embryo. *Proc. Natl. Acad. Sci. USA* **107**, 16160-16165.
Vallin, J., Thuret, R., Giacomello, E., Faraldo, M. M., Thiery, J. P. and Broders, F. (2001). Cloning and characterization of three Xenopus slug promoters reveal direct regulation by Lef/beta-catenin signaling. *J. Biol. Chem.* **276**, 30350-30358.
Wei, S. (2013). ADAM metalloproteinases. In *The Handbook of Proteolytic Enzymes* (ed. N. D. Rawlings and S. Guy), pp. 1086-1094. London, UK: Academic Press.
Wei, S., Whittaker, C. A., Xu, G., Bridges, L. C., Shah, A., White, J. M. and Desimone, D. W. (2010a). Conservation and divergence of ADAM family proteins in the Xenopus genome. *BMC Evol. Biol.* **10**, 211.
Wei, S., Xu, G., Bridges, L. C., Williams, P., White, J. M. and DeSimone, D. W. (2010b). ADAM13 induces cranial neural crest by cleaving class B Ephrins and regulating Wnt signaling. *Dev. Cell* **19**, 345-352.
Wei, S., Xu, G., Bridges, L. C., Williams, P., Nakayama, T., Shah, A., Grainger, R. M., White, J. M. and Desimone, D. W. (2012). Roles of ADAM13-regulated Wnt activity in early Xenopus eye development. *Dev. Biol.* **363**, 147-154.
Zhu, Q., Lu, Q., Gao, R. and Cao, T. (2016). Prospect of human pluripotent stem cell-derived neural crest stem cells in clinical application. *Stem Cells Int.* **2016**, 7695836.